Consideration of the boundary conditions represented by Eqs. (8) should be performed in a way similar to that shown above in the local coordinate system. The condition for the normal component yields

$$2\pi\nu(\boldsymbol{x}) + \int_\Gamma \frac{\nu(\boldsymbol{x})\boldsymbol{n}_x\boldsymbol{s}}{s^d}\,\mathrm{d}\Gamma(\boldsymbol{x}') + \mathrm{rot}_n\left[\boldsymbol{\Phi}(\boldsymbol{x}) + \int_\Gamma \boldsymbol{\mu}(\boldsymbol{x}')F(\boldsymbol{s})\,\mathrm{d}\Gamma(\boldsymbol{x}')\right]w_n = 0$$

The boundary conditions for the tangential components are

$$2\pi\mu_{t_1}(\boldsymbol{x}) + \int_\Gamma \frac{\mu_{t_1}(\boldsymbol{x}')\boldsymbol{n}_x\boldsymbol{s}}{s^d}\,\mathrm{d}\Gamma(\boldsymbol{x}') + \int_\Gamma \nu(\boldsymbol{x}')\frac{\partial F(\boldsymbol{s})}{\partial t_2}\,\mathrm{d}\Gamma(\boldsymbol{x}') - \int_\Gamma \mu_n(\boldsymbol{x}')\frac{\partial F(\boldsymbol{s})}{\partial t_1}\,\mathrm{d}\Gamma(\boldsymbol{x}') + \mathrm{rot}_{t_2}\boldsymbol{\Phi}(\boldsymbol{x}) - w_{t_2} = 0$$

$$2\pi\mu_{t_2}(\boldsymbol{x}) + \int_\Gamma \frac{\mu_{t_2}(\boldsymbol{x}')\boldsymbol{n}_x\boldsymbol{s}}{s^d}\,\mathrm{d}\Gamma(\boldsymbol{x}') - \int_\Gamma \nu(\boldsymbol{x}')\frac{\partial F(\boldsymbol{s})}{\partial t_1}\,\mathrm{d}\Gamma(\boldsymbol{x}') - \int_\Gamma \mu_n(\boldsymbol{x}')\frac{\partial F(\boldsymbol{s})}{\partial t_2}\,\mathrm{d}\Gamma(\boldsymbol{x}') - \mathrm{rot}_{t_1}\boldsymbol{\Phi}(\boldsymbol{x}) + w_{t_1} = 0$$

In a manner similar to that of the two-dimensional case, the boundary-condition problem is reduced to the system of Fredholm equations of the second kind. This system, together with the vorticity transport equations, represents the closed system of governing equations for the three-dimensional NS flows.

Concluding Remarks

The intent of this Note has been to highlight some aspects concerning the no-slip boundary conditions for the vorticity–velocity formulation or, more precisely, the $u-\omega$ integro-differential formulation, of the NS equations. This Note has shown that the problem of the boundary condition can be reduced to the system of Fredholm equations of the second kind. The solution of this system gives the distribution of vortices and sinks on the surface of the body; the integral representation of the solution with vorticities and sources yields the exact solution that meets the no-slip conditions.

Acknowledgments

The author is grateful to A. Pfeffer, the manager of the Power Fluid Dynamics Program, and Th. Sattelmayer, head of the Aerodynamic and Combustion Department, both of Aesa Brown Boveri, Ltd., Corporate Research Center, Daetwil, Switzerland, for numerous stimulating discussions and the permanent support that have finally led to the publication of this Note. The author also wish to thank J. Lloyd, who carefully read the manuscript and made important improvements.

References

[1]Gresho, P. M., "Incompressible Fluid Dynamics: Some Fundamental Formulation Issues," *Annual Review of Fluid Mechanics*, Vol. 23, 1991, pp. 413–453.

[2]Gatski, T. B., "Review of Incompressible Fluid Flow Computations Using the Vorticity–Velocity Formulation," *Applied Numerical Mathematics*, Vol. 7, 1991, pp. 227–239.

[3]Wu, J. C., "Numerical Boundary Conditions for Viscous Flow Problems," *AIAA Journal*, Vol. 14, No. 8, 1976, pp. 1042–1049.

[4]Wu, J. C., "Fundamental Solutions and Numerical Methods for Flow Problems," *International Journal for Numerical Methods in Fluids*, No. 4, 1984, pp. 185–201.

[5]Wu, J. C., and Gulcat, U., "Separate Treatment of Attached and Detached Flow Regions in General Viscous Flows," *AIAA Journal*, Vol. 19, No. 1, 1981, pp. 20–27.

[6]Wu, J. C., and Thomson, J. F., "Numerical Solutions of Time Dependent Incompressible Navier–Stokes Equations Using an Integro-Differential Formulation," *Computers and Fluids Journal*, Vol. 1, No. 2, 1973, pp. 197–215.

[7]Wang, C. M., and Wu, J. C., "Numerical Solution of Steady Navier–Stokes Problems Using Integral Representations," *AIAA Journal*, Vol. 24, No. 8, 1986, pp. 1305–1312.

[8]Wu, J. C., "Fundamental Solutions and Boundary Element Methods," *Engineering Analysis*, Vol. 4, No. 1, 1987, pp. 2–6.

[9]Vladimirov, V. S., *Equations of Mathematical Physics*, Nauka, Moscow, 1976, pp. 308–380 (in Russian).

Oblique-Shock/Expansion-Fan Interaction—Analytical Solution

H. Li* and G. Ben-Dor†
Ben-Gurion University of the Negev, Beer Sheva, Israel

Introduction

CONSIDER Fig. 1a, in which a supersonic flow having a Mach number M_0 flows inside a channel that suddenly turns by an angle δ_1. For the flow to negotiate this sudden turn, a centered expansion wave and an oblique shock wave are generated at the expansive and compressive corners, respectively, as shown in Fig. 1a. The oblique shock wave intersects the leading characteristic of the expansion fan at point A, initiating the interaction between these two waves. As a result, the slope of the oblique shock wave changes continuously until it emerges from the expansion fan at point B, which marks the intersection of the oblique shock wave with the tail of the expansion fan. Beyond point B the oblique shock wave is again straight. As shown in Fig. 1a it eventually reflects from the upper wall of the channel. Although the reflection shown in Fig. 1a is regular, a Mach reflection is also possible. The type of the reflection that actually occurs depends on both the aerodynamic and the geometric conditions. Upon crossing the curved portion of the oblique shock wave, the expansion waves are also bent, until they emerge from the slipstream and become straight. In Fig. 1a, the transmitted expansion waves are seen to reflect from the bottom wall of the channel.

Since the subject of this paper is the interaction between an oblique shock and a centered expansion fan, the subsequent interactions of the reflected shock and reflected expansion waves will not be considered here.

An interaction similar to the one shown in Fig. 1a takes place in a Mach reflection in steady flows, as shown in Fig. 1b. Here, the reflected shock wave R interacts with the centered expansion fan that is formed at the trailing edge of the reflecting wedge. The transmitted expansion waves interact then with the slipstream S and turns it away from the bottom surface. As a result a throat is formed in the flow tube formed by the bottom surface and the slipstream. According to Azevedo and Liu[1] the cross-sectional area of this throat determines the actual height of the Mach stem.

The interaction between an oblique shock and a centered expansion fan is observed in many other aerodynamic situations, e.g., a supersonic jet emanating from an overexpanded nozzle or the wave interaction associated with a ram accelerator, a device for accelerating projectiles to ultrahigh velocities. Surprisingly, however, it appears never to have been solved analytically. Consequently, the aim of the present study is such an analytical solution.

Present Study

The relevant flow states and flow parameters are defined in Fig. 1a together with the selected origin of the (x, y) coordinate system. State 0 is ahead of both the oblique shock and the centered expansion fan, state 2 is aft of the centered expansion fan, state 3 is aft of the transmitted oblique shock wave, and state 5 is obtained behind the oblique shock wave regularly reflected at point R. State 1 is reached just behind the oblique shock wave, and state 4 is aft of the transmitted expansion waves. Note that states 3 and 4, having different flow histories, are separated by a layer of varying entropy. The streamlines in these two flow states are parallel and the pressures are equal.

Received Jan. 11, 1995; revision received April 24, 1995; accepted for publication April 28, 1995.

*Ph.D. Student, Pearlstone Center for Aeronautical Engineering Studies, Department of Mechanical Engineering.

†Professor and Dean of Faculty of Engineering Sciences, Pearlstone Center for Aeronautical Engineering Studies, Department of Mechanical Engineering.

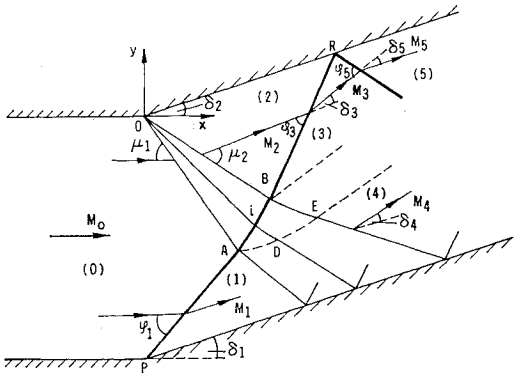

Fig. 1a Schematic illustration of the interaction between an oblique shock wave and a centered expansion fan that results when a supersonic flow is suddenly turned in a two-dimensional channel: φ—angle of incidence, δ—deflection angle, μ—Mach angle, M—flow Mach number, and 0 to 5—flow regions.

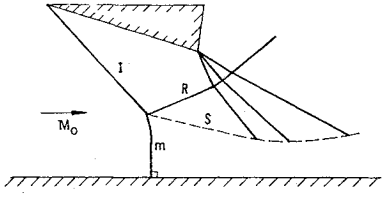

Fig. 1b Schematic illustration of the wave configuration of a steady Mach reflection. Note the interaction between the reflected shock wave and the centered expansion fan that is similar to that shown in Fig. 1a. *I*—incident shock wave, *R*—reflected shock wave, *M*—Mach stem, and *S*—slipstream.

The initial conditions of the interaction under consideration are the flow Mach number ahead of the oblique shock and centered expansion fan M_0, the flow deflection angle across the oblique shock wave δ_1, and the flow deflection angle across the centered expansion fan δ_2. In addition, the thermodynamic properties, e.g., pressure P_0 and speed of sound a_0, of state (0) are assumed to be known and the entire flow is assumed to be inviscid.

Governing Equations

Let us first consider the interaction between a shock wave and an infinitely weak discontinuity (e.g., a Mach wave) that occurs at point A of Fig. 1a. Note that the flow direction does not change when it passes through the weak discontinuity. However, owing to the fact that the orientation of the shock wave changes infinitesimally, a corresponding infinitesimal entropy difference between the streamlines above and below point A develops. As a result a weak tangential discontinuity shown by the dashed line in Fig. 1a, is created. The flow streamlines on both sides of this discontinuity are parallel and the pressures are equal.

The oblique shock wave relations are

$$\delta_1 = F(\gamma, M_0, \varphi_1) = \arctan\left[\frac{2\cot\varphi_1\left(M_0^2\sin^2\varphi_1 - 1\right)}{M_0^2(\gamma + \cos 2\varphi_1) + 2}\right] \tag{1}$$

$$M_1 = G(\gamma, M_0, \varphi_1) = \frac{\left(1+(\gamma-1)M_0^2\sin^2\varphi_1+\left\{[(\gamma+1)/2]^2 - \gamma\sin^2\varphi_1\right\}M_0^4\sin^2\varphi_1\right)^{\frac{1}{2}}}{\left[\gamma M_0^2\sin^2\varphi_1 - (\gamma-1)/2\right]^{\frac{1}{2}}\left[((\gamma-1)/2)M_0^2\sin^2\varphi_1 + 1\right]^{\frac{1}{2}}} \tag{2}$$

$$P_1/P_0 = W(\gamma, M_0, \varphi_1) = \frac{2\gamma M_0^2\sin^2\varphi_1 - (\gamma-1)}{\gamma+1} \tag{3}$$

and

$$a_1/a_0 = A(\gamma, M_0, \varphi_1) = \frac{\left[2\gamma M_0^2\sin^2\varphi_1 - (\gamma-1)\right]^{\frac{1}{2}}\left[(\gamma-1)M_0^2\sin^2\varphi_1 + 2\right]^{\frac{1}{2}}}{(\gamma+1)M_0\sin\varphi_1} \tag{4}$$

Here δ_1, M_1, P_1, and a_1 are the flow deflection angle, flow Mach number, pressure, and sound speed, respectively.

Similarly the flow Mach number M_2, the pressure P_2, and the speed of sound a_2 behind the centered expansion fan, shown schematically in Fig. 1a, can be obtained from

$$\nu(M_2) = \nu(M_0) + \delta_2 \tag{5}$$

where $\nu(M)$, the Prandtl–Meyer angle, is given by

$$\nu(M) = \left(\frac{\gamma+1}{\gamma-1}\right)^{\frac{1}{2}}\arctan\left[\left(\frac{\gamma-1}{\gamma+1}\right)(M^2-1)\right]^{\frac{1}{2}} - \arctan(M^2-1)^{\frac{1}{2}} \tag{5a}$$

and

$$P_2 = P_0[\Theta(\gamma, M_0, M_2)]^{\frac{\gamma}{\gamma-1}} \tag{6}$$

$$a_2 = a_0[\Theta(\gamma, M_0, M_2)]^{\frac{1}{2}} \tag{7}$$

where

$$\Theta(\gamma, M_0, M_2) = \left(1 + \frac{\gamma-1}{2}M_0^2\right)\Big/\left(1 + \frac{\gamma-1}{2}M_2^2\right)$$

The conditions in state 3, which, as shown in Fig. 1a, is obtained from the flow in state 2 while passing through the transmitted shock wave BR, can be calculated from the aforementioned oblique shock relations (the definition of the various parameters are given in Fig. 1a):

$$\delta_3 = F(\gamma, M_2, \varphi_3) \tag{8}$$

$$M_3 = G(\gamma, M_2, \varphi_3) \tag{9}$$

$$P_3/P_2 = W(\gamma, M_2, \varphi_3) \tag{10}$$

$$a_3/a_2 = A(\gamma, M_2, \varphi_3) \tag{11}$$

Similarly, the flow properties in state 4, which, as shown in Fig. 1a, is obtained from the flow in state 1 by passing through the transmitted expansion waves, can be calculated from the following relations (for definition see Fig. 1a):

$$\nu(M_4) = \nu(M_1) + \delta_4 \tag{12}$$

$$P_4 = P_1[\Theta(\gamma, M_0, M_2)]^{\frac{\gamma}{(\gamma-1)}} \tag{13}$$

(Note that the flow across the transmitted expansion waves is also isentropic.)

Since, as mentioned earlier, the streamlines in regions 3 and 4 are parallel, the matching conditions between regions 3 and 4 are

$$P_3 = P_4 \tag{14}$$

$$\delta_2 + \delta_3 = \delta_1 + \delta_4 \tag{15}$$

where δ_2 is known as an initial condition.

The preceding set of 15 equations consists of 15 unknowns, namely, P_1, P_2, P_3, P_4, M_1, M_2, M_3, M_4, a_1, a_2, a_3, φ_1, φ_3, δ_3, and δ_4, provided M_0, a_0, P_0, δ_1, δ_2, and γ are known. Consequently, this set of equations is complete and can, in principle, be solved.

Note that the angle of incidence of the oblique shock wave φ_1 is calculated from Eq. (1). However, Eq. (1) yields two mathematical roots for given values of M_0 and δ_1 provided δ_1 is smaller than the maximum deflection angle. Experimental observations indicate that the smaller of the two roots is the one that actually takes place.

Shape of the Curved Shock $\overline{AB}$

Owing to the nonlinearity of the problem under investigation it is impossible to get an exact analytical expression of the shape of the curved shock wave AB. However, under some simplifying assumptions an approximated analytical expression can, in fact, be

developed. Let us assume that the curved shock wave AB has a shape of a second-order polynomial, i.e.,

$$y = ax^2 + bx + c \tag{16}$$

At point A (see Fig. 1a) this relation should fulfill the following conditions:

$$y_A = ax_A^2 + bx_A + c \tag{17}$$

$$\left.\frac{dy}{dx}\right|_A = 2ax_A + b = \tan\varphi_1 \tag{18}$$

where $x_A = r_0 \cos\mu_1$ and $y_A = -r_0 \sin\mu_1$. Here r_0 is the length of the head of the centered expansion fan, i.e., OA in Fig. 1a, and its Mach angle μ_1 can be simply calculated from $\mu_1 = \arcsin(1/M_0)$. Similarly, at point B (see Fig. 1a) the relation given by Eq. (16) should fulfill the following conditions:

$$y_B = ax_B^2 + bx_B + c \tag{19}$$

$$\left.\frac{dy}{dx}\right|_B = 2ax_B + b = \tan(\varphi_3 + \delta_2) \tag{20}$$

where $x_B = r_1 \cos(\mu_2 - \delta_2)$ and $y_B = -r_1 \sin(\mu_2 - \delta_2)$. Here r_1 is the length of the tail of the centered expansion fan, i.e., OB in Fig. 1a, and its Mach angle μ_2 (see Fig. 1a) is given by $\mu_2 = \arcsin(1/M_2)$.

By solving Eqs. (17–20) one obtains

$$\frac{r}{r_0} = \frac{\sin(\mu_1 + \mu_2 - \delta_2) + [\tan\varphi_1 + \tan(\varphi_3 + \delta_2)]\cos(\mu_2 - \delta_2) - [\sin^2(\mu_1 + \mu_2 - \delta_2) - \sin 2\mu_1 \sin 2(\mu_2 - \delta_2)]}{\sin 2(\mu_2 - \delta_2) + [\tan\varphi_1 + \tan(\varphi_3 + \delta_2)]\cos^2(\mu_2 - \delta_2)} \tag{21}$$

and

$$a = \frac{\tan\varphi_1 - \tan(\varphi_3 + \delta_2)}{2r_0[\cos\mu_1 - (r/r_0)\cos(\mu_2 - \delta_2)]} \tag{22a}$$

$$b = \frac{\cos\mu_1 \tan(\varphi_3 + \delta_2) - (r/r_0)\cos(\mu_2 - \delta_2)\tan\varphi_1}{\cos\mu_1 - (r/r_0)\cos(\mu_2 - \delta_2)} \tag{22b}$$

$$c = -r_0(\cos\mu_1 \tan\varphi_1 + \sin\mu_1) + \frac{r_0\cos^2\mu_1[\tan\varphi_1 - \tan(\varphi_3 + \delta_2)]}{2[\cos\mu_1 - (r/r_0)\cos(\mu_2 - \delta_2)]} \tag{21}$$

Note that the shape of curved shock wave AB is known, and the intersection of any expansion characteristic line, e.g., point i in Fig. 1a, can be found by solving the following two equations:

$$y_i = -x_i \tan\eta_i \tag{23a}$$

$$y_i = ax_i^2 + bx_i + c \tag{23b}$$

Here η_i is the Mach angle of the corresponding expansive characteristic line. It is bounded by $\mu_1 \geq \eta_i \geq \mu_2 - \delta_2$.

Once the coordinates x_i and y_i at any point i along the curved shock wave AB are known, the shapes of the expansive characteristics of the transmitted expansion waves can be calculated again, assuming that they can be described by second-order polynomials.

The shape of the transmitted expansion wave is very important if one is to consider its interaction with the slipstream of the Mach reflection shown in Fig. 1b. As mentioned previously, this interaction eventually forms the throat in the flow tube bounded by the bottom wall and the slipstream. The area of this throat controls the height of the Mach stem, in particular, and the entire Mach reflection size, in general.[1]

Reflection of the Transmitted Shock Wave from the Upper Wall

As mentioned earlier, the transmitted shock wave (BR in Fig. 1a) can reflect from the upper wall either as a regular reflection (RR), as shown in Fig. 1a, or as a Mach reflection (MR), depending on both the initial gasdynamic and the geometrical conditions.

Two RR $\Leftrightarrow$ MR transition criteria exist in steady flows. They are known as the "detachment" D and the "von Neumann" N conditions.[2,3] Based on these two transition criteria it is obvious that if $\varphi_3 < \varphi_3^N$ the reflection is an RR; if $\varphi_3 > \varphi_3^D$ the reflection is an MR, and if $\varphi_3^N \leq \varphi_3 \leq \varphi_3^D$ then both RR and MR are theoretically possible.

Regular Reflection

If the transmitted shock wave reflects as a regular reflection, as shown in Fig. 1a, then the angle φ_5 and the flow Mach number M_5 could be simply calculated from

$$\delta_3 = F(\gamma, M_3, \varphi_5) \tag{24}$$

$$M_5 = G(\gamma, M_3, \varphi_5) \tag{25}$$

where δ_3 and M_3 were calculated by solving Eqs. (1–15).

Mach Reflection

If the transmitted shock wave reflects as a Mach reflection, a solution similar to that shown in the previous section for the case of an RR is impossible. This is because the length of the Mach stem, behind which the flow is subsonic, is determined by downstream conditions.

Analytical Results

In the following some analytical results that were obtained by solving the problem shown in Fig. 1a are presented. Unfortunately, the lack of such detailed experimental data does not allow validation of the analytical predictions.

The analytical results for the combination of three deflection angles δ_1 and various incident flow Mach numbers M_0 are shown in Table 1. The minimum incident flow Mach number M_0^{det} for which the incident oblique shock is attached is indicated for each value of δ_1. The difference in the orientations of the transmitted and the oblique shock waves β is indicated by $\beta = \delta_2 + \varphi_3 - \varphi_1$. The terms M_3 and M_4 are the flow Mach numbers in regions 3 and 4, respectively, which exist on the opposite sides of the layer of varying entropy. It is evident from Table 1 that β increases as M_0 increases for a given value of δ_1.

An inspection of the analytical values of M_3 and M_4 indicates that $M_3 < M_0 < M_4$. For the smallest value of δ_1, i.e., $\delta_1 = 5$ deg, $(M_3 + M_4)/2 \approx M_0$. A slight rearrangement of Table 1 results in Table 2, from which it is clearly seen that β increases as δ_1 increases for a given value of M_0.

Table 1 Predicted analytical results

δ_1	M_0	β, deg	M_3	M_4
5 deg, $M_0^{det} = 1.23$	1.5	0.08	1.47	1.53
	2.0	3.05	1.95	2.04
	3.0	4.39	2.92	3.07
	5.0	5.03	4.80	5.15
15 deg, $M_0^{det} = 1.60$	2.0	9.47	1.79	2.09
	3.0	15.09	2.56	3.16
	5.0	19.41	3.52	5.34
25 deg, $M_0^{det} = 2.04$	2.5	26.14	1.54	2.63
	3.5	35.90	1.63	3.79
	5.0	47.63	1.41	5.71

Table 2 Predicted analytical results

M_0	δ_1, deg	β, deg
2.0	5	3.05
	15	9.47
3.0	5	4.39
	15	15.09
5.0	5	5.03
	15	19.41
	25	47.63

Conclusions

The governing equations describing the flowfield that results from the interaction of a centered expansion fan with an oblique shock wave in steady flows were formulated and solved analytically for a perfect inviscid gas.

Since, as mentioned in the Introduction, the interaction of a centered expansion fan with an oblique shock wave is encountered in many steady flowfields, the model developed in the course of this study could assist in investigating these flowfields and improve our understanding of the effect of the various parameters associated with them.

References

[1]Azevedo, D. J., and Liu, S. L., "Engineering Approach to the Prediction of Shock Patterns in Bounded High-Speed Flows," *AIAA Journal*, Vol. 31, 1993, pp. 83–93.

[2]Ben-Dor, G., *Shock Wave Reflection Phenomena*, Springer–Verlag, New York, 1991, Chap. 3.

[3]Ben-Dor, G., "Reconsideration of the State-of-the-Art of the Shock Wave Reflection Phenomenon in the Steady Flows," *JSME International Journal* (to be published).

Automation of Some Operations of a Wind Tunnel Using Artificial Neural Networks

Arthur J. Decker* and Alvin E. Buggele†
NASA Lewis Research Center,
Cleveland, Ohio 44135-3191

Introduction

ARTIFICIAL neural networks have been tested as components for automating wind-tunnel operations in a 3.81 × 10 in. (0.0968 × 0.254 m) subsonic/transonic/supersonic wind tunnel at NASA Lewis Research Center. The authors previously reported an approach to automation[1,2] that uses operator-trained, workstation-resident neural nets as sequencers. Briefly stated, a sequencer estimates for a wind tunnel information such as the next appropriate control settings, flow visualization patterns, or sensor values from the current control settings, flow visualization patterns, or sensor values. The authors intend eventually to have these estimates transmitted, after encoding, to an existing, commercial, programmable logic control system[3] to set the next appropriate state of the tunnel without human intervention. This approach is selected to be minimally intrusive on existing Lewis control systems that accept soft commands. Further discussions and explanations of the theory, the development, and the applications of neural networks, including different uses for control, are left to the extensive literature. A few general references are cited.[4–6]

Artificial neural networks were trained and tested at NASA Lewis Research Center for estimating sensor readings from shadowgraph patterns, shadowgraph patterns from shadowgraph patterns, and sensor readings from sensor readings. This Note will discuss only the results of estimating sensor readings from shadowgraph patterns. Human operators routinely adjust and change, for example, pressure values after viewing flow visualization patterns.

The tunnel was operated with its Mach 2.0 nozzle for this work. Shadowgraph was recorded with a continuous light source and a charge-coupled device (CCD) camera near the nozzle exit. The human operator operated the controls and created the training examples from this mode of flow visualization. The next section discusses the tunnel and its information handling systems.

Operational Procedure and Information Handling

The wind tunnel used to generate the training sets for the neural-net sequencers was actually an upgrade of the first supersonic wind tunnel operated at Lewis Research Center (circa 1946).[7] The highly simplified diagram of Fig. 1 shows the specific components of the tunnel needed to interpret the operational procedure and results. The combustion air valves AC-2408 A and AC-2408 B essentially control the flow. The groups of boundary-layer bleed and exhaust valves were preset for training set generation. In fact, any serious attempt at complete automation would eventually need to recognize that the tunnel uses more than 60 valves.

Flow visualization was acquired through a pair of 47-in. (1.19-m) long windows. The shadowgraph field for this work was actually centered near the right edges of the windows 40 in. (1.02 m) downstream of the nozzle throat or approximately 2 in. (0.05 m) downstream of the nozzle exit. The positional stability and repeatability of the one-pass shadowgraph and the tunnel wall were assured to within 0.002 in. (0.005 cm) using a hard mounted system with taper dowel pins. The actual shadowgraph field recorded was about 10 × 8.5 in. (0.25 × 0.21 m). A sample image is inserted in Fig. 1 for reference.

Figure 1 shows only three of many sensors. The static inlet or plenum pressure is indicated by P_7, and a static test section pressure located 0.5 in. (1.27 cm) downstream of the nozzle exit is indicated by P_8. The Mach number probe MN_3 was located 48 in. (1.22 m) aft of the nozzle throat or about 8 in. (0.2 m) downstream of the

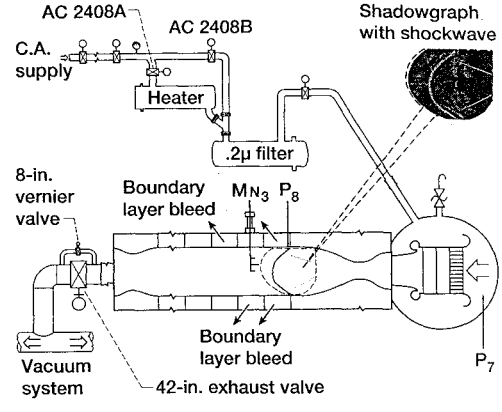

Fig. 1 Tunnel components and shadowgraph field.

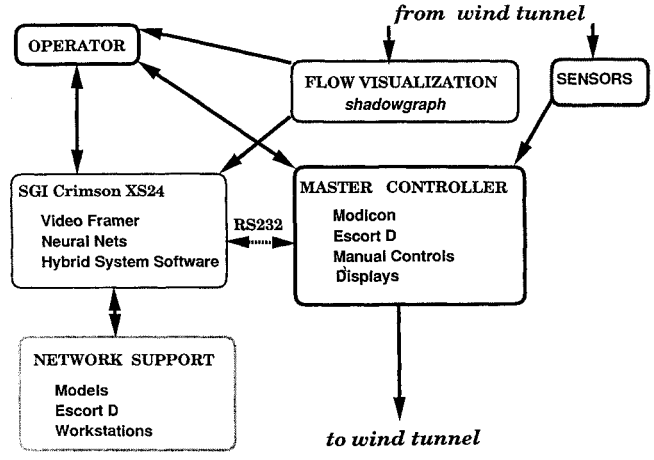

Fig. 2 Flow of information handling and control.

Received April 24, 1995; revision received Sept. 21, 1995; accepted for publication Oct. 9, 1995.

*Senior Research Scientist, Instrumentation and Control Technology Division, 21000 Brookpark Road.

†Senior Operations Engineer, Aeropropulsion Facilities and Experiments Division, 21000 Brookpark Road. Senior Member AIAA.